

Calculation of band bending in ferroelectric semiconductor

Hideharu Matsuura

Department of Electronics, Osaka Electro-Communication University,
18-8 Hatsu-cho, Neyagawa, Osaka 572-8530, Japan

E-mail: matsuura@isc.osakac.ac.jp

<http://www.osakac.ac.jp/labs/matsuura/>

New Journal of Physics **2** (2000) 8.1–8.11 (<http://www.njp.org/>)

Received 24 September 1999; online 14 April 2000

Abstract. In order to investigate the electronic characteristics of ferroelectric thin films that behave as semiconductors, we derive an equation to calculate the band bending in ferroelectrics, to replace the Poisson equation. We find that the space-charge density term, ρ , in the Poisson equation should be replaced by $\rho - \nabla P_r$, where P_r is the remanent polarization. In order to simplify the band bending calculation, only one dimension is considered here. For example, in the case of the 3 V band bending in a metal–semiconductor Schottky barrier junction with a 1 μm thick ferroelectric semiconductor, the depletion region extends over the whole semiconductor, even with a dielectric constant of 10 and a donor density of $1 \times 10^{17} \text{ cm}^{-3}$ due to dP_r/dx . However, the depletion layer width in a semiconductor without remanent polarization is only about 0.18 μm under the same conditions.

1. Introduction

Researchers investigating nonvolatile memory elements in large-scale integrated circuits (LSIs) are interested in ferroelectrics [1]–[3]. In a metal–ferroelectric–metal (MFM) capacitor, the electric field is considered to be uniform over the whole film when the voltage is applied to the capacitor, because the ferroelectric film is regarded as an insulator. As a result, the remanent polarization is constant in the ferroelectric film. Since the remanent polarization cannot cancel out at both metal–ferroelectric interfaces, the remanent polarization appears only at the interfaces.

Ferroelectrics such as barium titanate (BaTiO_3) and lead–lanthanum–zirconate–titanate (PLZT) have a wide bandgap of 3–4 eV [4]–[7], and dielectrics such as strontium titanate (SrTiO_3), with structures similar to BaTiO_3 , have previously been treated as wide bandgap semiconductors [7]. Therefore, ferroelectrics should be considered as behaving like semiconductors with wide bandgaps, indicating that the electric field should no longer be constant

over the whole ferroelectric film. For example, when the imprint phenomena in MFM capacitors are interpreted, their metal–ferroelectric contacts are considered to be equivalent to the metal–semiconductor Schottky barrier junction [8].

On the other hand, wide bandgap semiconductors such as silicon carbide (SiC), diamond and gallium nitride (GaN) have recently been regarded as promising semiconductors for high-power electronic applications. Since many researchers have intensively studied the growth of single crystalline ferroelectric thin films with wide bandgaps [9], they are very likely to be successfully grown in the near future. These ferroelectric semiconductors will make the creation of new electronic devices possible. To make use of ferroelectric semiconductors in electronic devices, it is therefore necessary to simulate the electronic characteristics of these devices.

The Poisson equation and the continuity equation are necessary to simulate the electronic characteristics of devices for semiconductors without remanent polarization (referred to as normal semiconductors here). The band bending in semiconductors strongly affects the current–transport mechanism and the capacitance in devices. In order to calculate the band bending in the depletion region for a normal semiconductor, we make use of the Poisson equation [10, 11]

$$\nabla^2 V = -\frac{\rho}{\epsilon_0 \epsilon_r} \quad (1)$$

where V is the potential difference corresponding to the band bending, and $V = 0$ V in the bulk. Here, ρ is the space–charge density in the semiconductor, ϵ_0 is the permittivity of free space, and ϵ_r is the dielectric constant of the semiconductor. However, in order to take account of the remanent polarization in ferroelectric semiconductors, the Poisson equation should be modified.

In this article, we derive an equation to calculate the band bending in ferroelectric semiconductors. We also discuss the difference between two kinds of band bending, calculated by the Poisson equation and the equation derived here, in a Schottky barrier junction (i.e. a metal–semiconductor contact).

2. Equation for calculating band bending in ferroelectric semiconductors

The first Maxwell equation

$$\nabla D = \rho \quad (2)$$

relates the electric flux density (D)

$$D = \epsilon_0 E + P \quad (3)$$

to the space-charge density given by

$$\rho = e (N_D^+ - N_A^- + p - n) \quad (4)$$

where E is the electric field, P is the polarization, e is the magnitude of the electron charge, N_D^+ is the ionized donor density, N_A^- is the ionized acceptor density, p is the hole concentration in the valence band, and n is the electron concentration in the conduction band. With $E = -\nabla V$, we obtain the equivalent of the Poisson equation

$$\nabla^2 V = -\frac{1}{\epsilon_0} (\rho - \nabla P). \quad (5)$$

In a ferroelectric semiconductor, the polarization is related to E by

$$P = P_r + \epsilon_0 \chi E \quad (6)$$

where P_r is the remanent polarization and χ is the electric susceptibility of the ferroelectric semiconductor. From equation (5), we obtain

$$\nabla^2 V = -\frac{1}{\epsilon_0 \epsilon_r} (\rho - \nabla P_r) \quad (7)$$

for a ferroelectric semiconductor. Here, we have assumed that the dielectric constant

$$\epsilon_r = 1 + \chi \quad (8)$$

is independent of P_r . Formula (7) can be applied generally to semiconductors and insulators. Since normal semiconductors have no remanent polarization, formula (7) is a form of the Poisson equation.

3. Remanent polarization in the depletion region of ferroelectric semiconductors

In order to investigate the influence of ∇P_r on the band bending, the simple relationship between P and E , shown in figure 1, is considered.

P_{rmax} and E_{cmax} represent the remanent polarization and the coercive field in the saturated polarization–electric field (P – E) hysteresis loop, respectively.

At first, P_r is assumed to vanish. As the figure shows, the value of P increases with increasing E as

$$P = \left(\epsilon_0 \chi + \frac{P_{rmax}}{E_{cmax}} \right) E. \quad (9)$$

After the electric field of E_c is applied to the semiconductor, the value of P obeys the following relation at $-E_c \leq E \leq E_c$

$$P = P_r + \epsilon_0 \chi E$$

where P_r is determined by E_c as

$$P_r = \frac{P_{rmax}}{E_{cmax}} E_c \quad (10)$$

at $E_c < E_{cmax}$. P_r does not change until $|E|$ exceeds $|E_c|$. Therefore, when the bias voltage is quasi-statically applied to the semiconductor (called the quasi-static application), E_c in equation (10) is equal to E . In the depletion region of the junction, E created by ionized dopants is inhomogeneous, which breaks the symmetry. Therefore, P_r is inhomogeneous in the depletion region, indicating that $\nabla P_r \neq 0$.

4. Charge density in semiconductors

Figure 2 shows the energy band diagram for the Schottky barrier junction that consists of an n-type semiconductor and metal. In the figure, E_C , E_F , E_D and E_V are the energy level at the bottom of the conduction band, the Fermi level, the donor level, and the energy level at the top of the valence band. The spatial dependence of the conduction electron concentration is displayed as $n(x)$ and n_0 is its value deep in the bulk. The potential $V(x)$ is measured with respect to E_C and is defined as zero in the bulk. Therefore, $V(x)$ is negative when the reverse bias is applied. In order to easily understand the effect of ∇P_r on the band bending, we consider only one type of donor, $N_A = 0$ and $p \ll n$ in the following discussion.

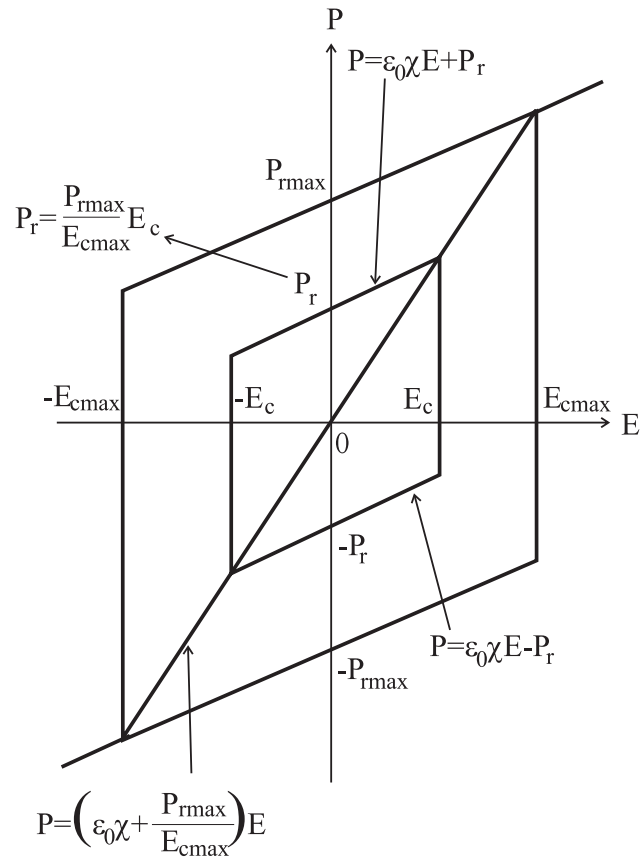


Figure 1. Schematic relationship between the polarization and the electric field in the ferroelectric semiconductor. The inner loop represents an unsaturated hysteresis loop when some $|E|$ lower than E_{cmax} is applied to a sample whose polarization is assumed to vanish. The outer loop represents the saturated hysteresis loop once $|E|$ becomes greater than or equal to E_{cmax} . P_{rmax} and E_{cmax} represent the remanent polarization and the coercive field in the saturated polarization–electric field (P – E) hysteresis loop, respectively.

In the bulk of the semiconductor, charge neutrality must exist, indicating that

$$\rho(x) = 0 \quad (11)$$

and

$$V(x) = 0. \quad (12)$$

From equation (4), therefore, we obtain

$$n_0 = N_D^+ \quad (13)$$

$$= N_D \left[1 - \frac{1}{1 + \exp\left(\frac{E_D - E_F}{kT}\right)} \right] \quad (14)$$

where k is the Boltzmann constant and T is the absolute temperature [10, 11].

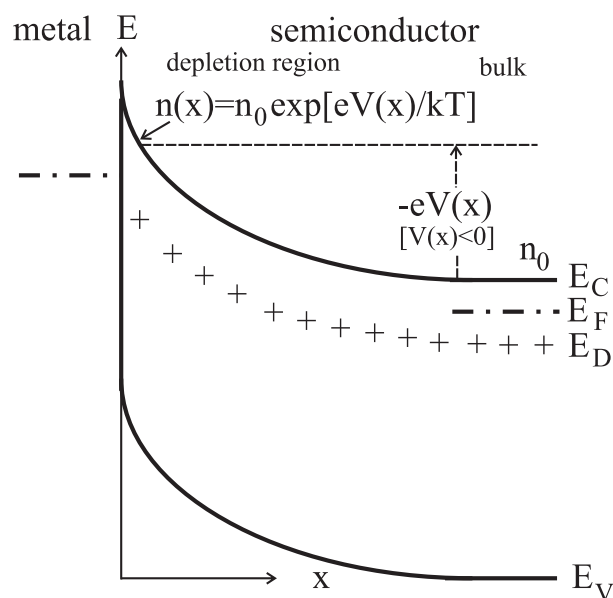


Figure 2. Energy band diagram for a Schottky barrier junction that consists of an n-type semiconductor and metal. The potential $V(x)$, defined as zero in the bulk, is measured with respect to E_C in the bulk. Therefore, $V(x)$ is negative when the reverse bias is applied.

In the depletion region, $n(x)$ is expressed as [11]

$$n(x) = n_0 \exp \left[\frac{eV(x)}{kT} \right] \quad (15)$$

$$= N_D \exp \left[\frac{eV(x)}{kT} \right] \quad (16)$$

when all donors are ionized in the bulk. From equation (4), therefore, we obtain

$$\rho(x) = eN_D \left\{ 1 - \exp \left[\frac{eV(x)}{kT} \right] \right\}. \quad (17)$$

5. Approximate estimation of depletion layer width

Using the depletion approximation (i.e. $\rho(x) = eN_D$ in the depletion region and $\rho(x) = 0$ in the bulk) [11], we can solve the Poisson equation easily. In the depletion region ($x < W$)

$$V(x) = V(0) \left(\frac{x - W}{W} \right)^2 \quad (18)$$

where W is the depletion layer width, given by

$$W = \sqrt{\frac{2\epsilon_0\epsilon_r[-V(0)]}{eN_D}} \quad (19)$$

and $V(0) < 0$. In the bulk ($x \geq W$), on the other hand, $V(x) = 0$.

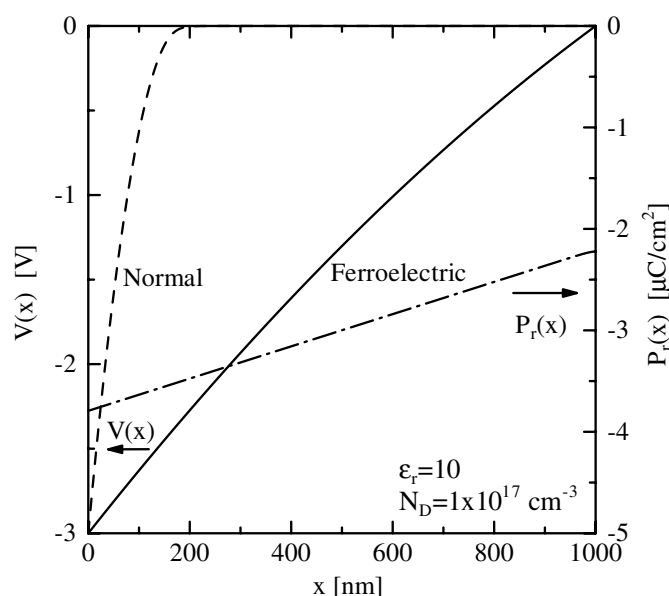


Figure 3. $V(x)$ profiles (broken and solid lines) corresponding to the normal and ferroelectric semiconductors, respectively, and $P_r(x)$ profile (dashed–dotted line) in the ferroelectric semiconductor.

If the depletion layer is wider than the sample thickness (d), the solution is

$$V(x) = V(0) \left[1 - \frac{x}{d} + \frac{x(x-d)}{W^2} \right] \quad (20)$$

because $\rho(x) = eN_D$ in the sample.

6. Results and discussion

We consider n-type ferroelectric semiconductors with $P_{r\max} = 10 \mu\text{C cm}^{-2}$ and $E_{c\max} = 100 \text{ kV cm}^{-1}$ and n-type normal semiconductors, and $d = 1 \mu\text{m}$. Using equation (17) and the one-dimensional formula

$$\frac{d^2V(x)}{dx^2} = -\frac{1}{\epsilon_0\epsilon_r} \left[\rho(x) - \frac{dP_r(x)}{dx} \right] \quad (21)$$

derived from equation (7), we calculate the band bending.

A reverse bias voltage is quasi-statically applied to a metal–semiconductor Schottky barrier junction. The contact at $x = 0$ is the Schottky barrier contact, and the contact at $x = d$ is an ohmic contact. The band bending is calculated under the conditions of $V(0) = -3 \text{ V}$ and $V(d) = V(0) - 3 \text{ V}$.

First, the effect of ϵ_r on the depletion layer width is investigated. Figure 3 shows the $V(x)$ profiles in the normal (broken line) and ferroelectric (solid line) semiconductors with $\epsilon_r = 10$ and $N_D = 1 \times 10^{17} \text{ cm}^{-3}$, and also shows the $P_r(x)$ profile (dashed–dotted line) in the ferroelectric semiconductor. The depletion region extends over the whole ferroelectric semiconductor, while

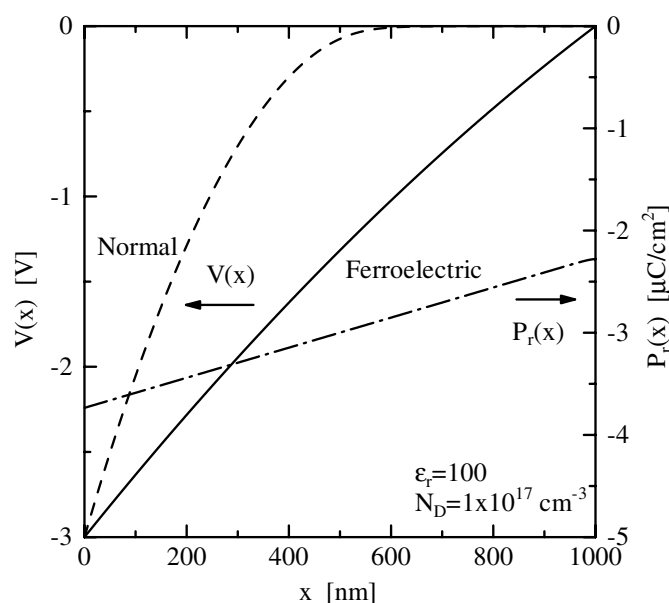


Figure 4. $V(x)$ profiles (broken and solid lines) corresponding to the normal and ferroelectric semiconductors, respectively, and the $P_r(x)$ profile (dashed–dotted line) in the ferroelectric semiconductor.

W in the normal semiconductor is only approximately 180 nm. It seems that the ferroelectric semiconductor behaves like a semiconductor with a very large dielectric constant

$$\epsilon_{r,\text{eff}} = \epsilon_r + \frac{P_{r\text{max}}}{\epsilon_0 E_{c\text{max}}} \quad (22)$$

during the increase of the remanent polarization, where $\epsilon_{r,\text{eff}}$ is derived using equation (8) and the effective χ that is derived from equation (9). From the viewpoint of the underlying physics, however, dP_r/dx indeed makes the depletion layer width wider, as equation (21) clearly shows.

As a result, the capacitances of the junctions are 49 nF cm^{-2} and 8.9 nF cm^{-2} for the normal and ferroelectric semiconductors, respectively. Therefore, the capacitance–voltage (C – V) characteristics for the ferroelectric semiconductor should be quite different from those for the normal semiconductor.

When both contacts in the metal–ferroelectric semiconductor–metal (MSM) diode are Schottky barrier junctions, the leakage current of the MSM diode is as low as that of a metal–insulator–metal (MIM) capacitor. Although the capacitance of the MIM capacitor is independent of the applied voltage, the capacitance of the MSM diode decreases with an increase in the absolute applied voltage. This is because the depletion layer width in the MSM diode increases on the side of the reverse biased junction. Moreover, since a high $E(x)$ is necessary to change $P_r(x)$, hysteresis appears in the C – V characteristics.

Figure 4 shows the $V(x)$ profiles in the normal (broken line) and ferroelectric (solid line) semiconductors with $\epsilon_r = 100$. The figure also shows the $P_r(x)$ profile (dashed–dotted line) in the ferroelectric semiconductor. Although W in the normal semiconductor is about 700 nm, the depletion region spreads over the whole ferroelectric semiconductor due to the effect of $dP_r(x)/dx$. In the ferroelectric semiconductors, the profiles of $V(x)$ and $P_r(x)$ in figure 4 are

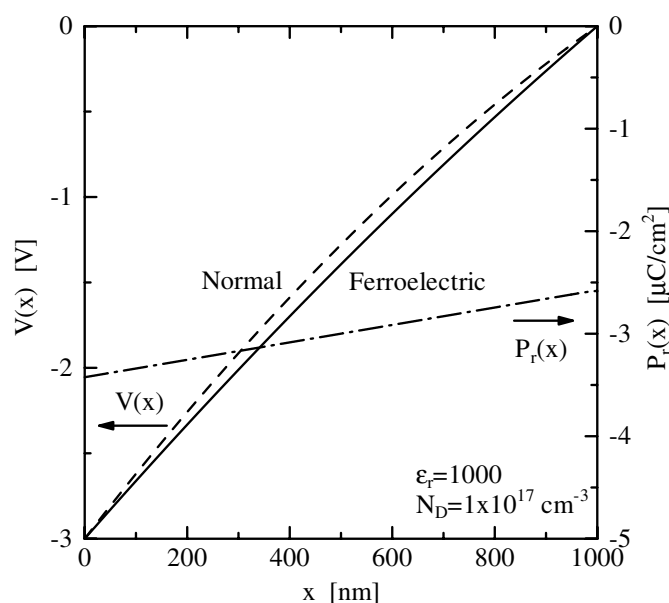


Figure 5. $V(x)$ profiles (broken and solid lines) corresponding to the normal and ferroelectric semiconductors, respectively, and the $P_r(x)$ profile (dashed–dotted line) in the ferroelectric semiconductor.

quite similar to those in figure 3, respectively, which insists that $dP_r(x)/dx$ strongly affects the band bending in these ferroelectric semiconductors.

Figure 5 shows the $V(x)$ profiles in the normal (broken line) and ferroelectric (solid line) semiconductors with $\epsilon_r = 1000$, and also shows the $P_r(x)$ profile (dashed–dotted line) in the ferroelectric semiconductor. The difference between the $V(x)$ profiles in the normal and ferroelectric semiconductors decreases, and the change in $P_r(x)$ is also smaller, compared with those in figures 3 and 4. Therefore, the effect of $dP_r(x)/dx$ on the band bending weakens.

Second, the effect of N_D on the depletion layer width is investigated. Figure 6 shows the $V(x)$ profiles in the normal (broken line) and ferroelectric (solid line) semiconductors, and the $P_r(x)$ profile (dashed–dotted line) in the ferroelectric semiconductor, where $\epsilon_r = 100$ and $N_D = 1 \times 10^{15} \text{ cm}^{-3}$. The depletion layer width in the normal semiconductor is calculated to be approximately 5800 nm from equation (19), which means that the depletion region should expand over the whole normal semiconductor. On the other hand, $P_r(x)$ is almost independent of x , suggesting that $dP_r(x)/dx \simeq 0$. Therefore, $\rho(x)$ determines the band bending in the ferroelectric semiconductor, just like in the normal semiconductor.

Finally, we consider the $V(x)$ profile when a reverse bias voltage is rapidly applied to the junction (known as the step-functional application). In figure 7, the broken lines represent the $V(x)$ and $P_r(x)$ profiles with $\epsilon_r = 10$ and $N_D = 1 \times 10^{17} \text{ cm}^{-3}$ for the step-functional application. The solid lines represent the $V(x)$ and $P_r(x)$ profiles for the quasi-static application, which are the same as those in figure 3.

The band bending does not reach a steady state after the reverse bias voltage is applied until the dielectric relaxation time ($\epsilon_0 \epsilon_r \rho_{\text{bulk}}$) has elapsed [12, 13] (ρ_{bulk} is the resistivity of the ferroelectric semiconductor in the bulk). This means that, initially, the constant electric field of -30 kV cm^{-1} is applied to the ferroelectric semiconductor before the band bending reaches a

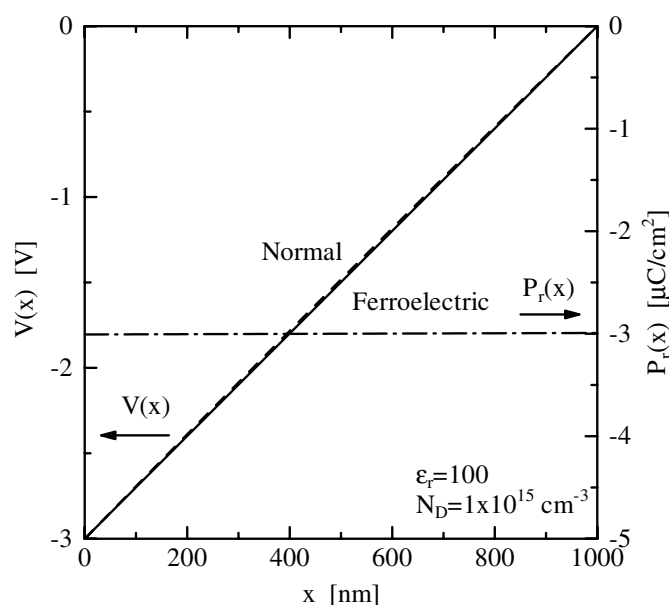


Figure 6. $V(x)$ profiles (broken and solid lines) corresponding to the normal and ferroelectric semiconductors, respectively, and $P_r(x)$ profile (dashed–dotted line) in the ferroelectric semiconductor.

steady state. Therefore, $P_r(x)$ at every x initially becomes $-3 \mu\text{C cm}^{-2}$, which is calculated from equation (10). As is clear from figure 7, the $P_r(x)$ profile (broken line) is constant at $-3 \mu\text{C cm}^{-2}$ when x is larger than about 810 nm, indicating that the $V(x)$ profile should obey the Poisson equation in this region. This case makes it clear that the band bending is strongly dependent on $dP_r(x)/dx$, and not $\epsilon_{r,\text{eff}}$. In all cases, therefore, formula (7) is found to be useful for calculating the band bending in semiconductors.

The above discussion is important when we study the current–voltage (I – V) and C – V characteristics of Schottky barrier junctions or p–n junctions. Since the depletion region in ferroelectric semiconductors is much wider than that in normal semiconductors, due to ∇P_r , the collisions of electrons (or holes) within the depletion region can no longer be neglected. For example, in Schottky barrier junctions, the current–transport mechanism should not result from the thermionic emission process [14, 15]. According to the diffusion theory [14], the current strongly depends on the band bending. On the other hand, when an AC bias voltage is applied to the junction, the band bending at the increasing bias is different from the band bending at the decreasing bias, because P_r changes only when $|E|$ exceeds $|E_c|$. Therefore, the I – V characteristics may exhibit hysteresis. Simulation of the electronic characteristics of various devices is in progress.

7. Conclusion

Since ferroelectric thin films have been regarded as insulators, the electric field was considered to be uniform over the whole film. However, because these films behave more like semiconductors, the electric field is not uniform in the film. Therefore, the effect of ∇P_r on the band bending in ferroelectric semiconductors has been investigated. In contrast with the Poisson equation,

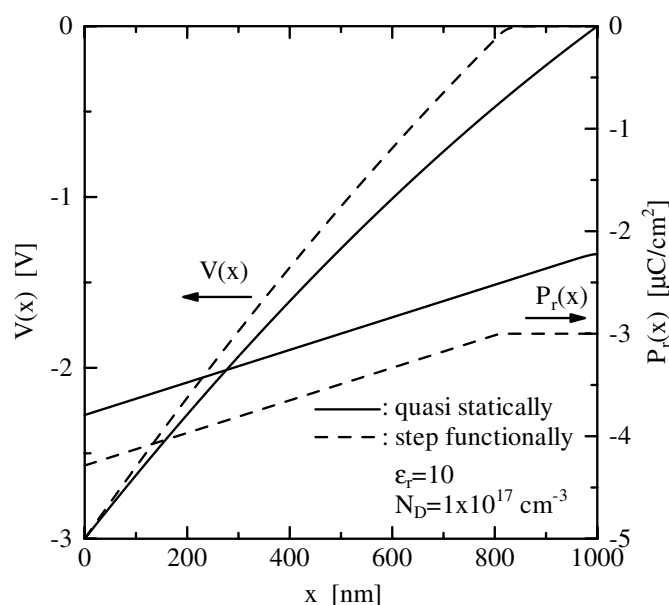


Figure 7. $V(x)$ profiles and $P_r(x)$ profiles corresponding to step-functional (broken lines) and quasi-static (solid lines) applications to the metal–ferroelectric semiconductor Schottky barrier junction.

the newly derived formula indicates that ∇P_r also affects the band bending in ferroelectric semiconductors, rather than just ρ . The difference between the band bending calculated from the Poisson equation and the newly derived formula has been discussed. In the saturated polarization–electric field hysteresis loop, the remanent polarization and the coercive field of 1 μm thick ferroelectric semiconductors were assumed to be 10 $\mu\text{C cm}^{-2}$ and 100 kV cm^{-1} , respectively. In the case of the band bending of 3 V in a metal–semiconductor Schottky barrier junction, the depletion region extended over the whole 1 μm thick ferroelectric semiconductor with values of $\epsilon_r = 10$ and $N_D = 1 \times 10^{17} \text{ cm}^{-3}$. However, the depletion layer width in the semiconductor without remanent polarization was only about 0.18 μm with the same values of ϵ_r and N_D . Our result suggests that the electronic junction properties of ferroelectric semiconductors should be reconsidered, using the band bending calculated by the formula derived here, instead of the Poisson equation.

References

- [1] Moll J L and Tarui Y 1963 *IEEE Trans. Electron Devices* **ED10** 328
- [2] Araujo C P, Scott J F and Taylor G W 1996 in *Ferroelectric Thin Films: Synthesis and Basic Properties* ed C P Araujo, J F Scott and G W Taylor (Amsterdam: Gordon and Breach) ch 1
- [3] See, for example
Special issue: ferroelectric materials and their applications 1998 *Japan. J. Appl. Phys.* **37** issue 9B
- [4] Eror N G and Smyth D M 1978 *J. Solid State Chem.* **24** 235
- [5] Choi G M, Tuller H L and Goldschmidt D 1986 *Phys. Rev. B* **34** 6972
- [6] Dimos D, Warren W L, Sinclair M B, Tuttle B A and Schwartz R W 1994 *J. Appl. Phys.* **76** 4305

8.11

- [7] Waser R and Smyth D M 1996 in *Ferroelectric Thin Films: Synthesis and Basic Properties* ed C P Araujo, J F Scott and G W Taylor (Amsterdam: Gordon and Breach) ch 3
- [8] Shimada Y, Inoue A, Nasu T, Nagano Y, Matsuda A, Arita K, Uemoto Y, Fujii E and Otsuki T 1996 *Japan. J. Appl. Phys.* **35** 4919
- [9] Auciello O, Krauss A R and Grifford K D (ch 10)
Krupanidhi S B, Hu H and Fox G R (ch 11)
Keijser M, Dormans G J M and Larsen P K (ch 12)
Auciello O, Dat R and Ramesh R (ch 13)
1996 *Ferroelectric Thin Films: Synthesis and Basic Properties* ed C P Araujo, J F Scott and G W Taylor, Part III (Amsterdam: Gordon and Breach)
- [10] Sze S M 1981 *Physics of Semiconductor Devices* 2nd edn (New York: Wiley) ch 1 and 2
- [11] Mouthaan T 1999 *Semiconductor Devices Explained Using Active Simulation* (New York: Wiley) ch 1 and 2
- [12] Matsuura H 1988 *J. Appl. Phys.* **64** 1964
- [13] Matsuura H and Okushi H 1992 *Amorphous & Microcrystalline Semiconductor Devices: Materials and Device Physics* ed J Kanicki (Boston: Artech House) ch 11, p 535
- [14] Rhoderick E H 1980 *Metal–Semiconductor Contacts* (Oxford: Oxford University Press) ch 3
- [15] Matsuura H and Okushi H 1987 *J. Appl. Phys.* **62** 2871